Preclinical evaluation of a handheld theranostic intraoral device for image-guided PDT treatment of pre-malignant and malignant oral lesions

Shakir Khan[a, b], Bofan Song[c], Sergio Farias[a], Rongguang Liang[c], Tayyaba Hasan[b, d], and Jonathan P. Celli[a, b]

[a]Department of Physics, College of Science and Mathematics, University of Massachusetts Boston, Boston, Massachusetts, United States.
[b]Massachusetts General Hospital, Harvard Medical School, Boston, Massachusetts, United States.
[c]The University of Arizona, Wyant College of Optical Sciences, Tucson, Arizona, United States.
[d]Division of Health Sciences and Technology, Harvard University and Massachusetts Institute of Technology, Cambridge, Massachusetts, United States.

ABSTRACT

Significance: Oral squamous cell carcinoma (OSCC) has an exceptionally high rate of incidence and mortality in India, with 15 cases per 100,000 people and over 70,000 deaths annually. The problem is exacerbated due to insufficient medical infrastructure for widescale screening and oncology care, particularly in rural regions. New technologies are urgently needed to detect oral cancer and provide timely treatment at the point of care. This work draws upon previous development and clinical validation of low-cost hardware for photodynamic therapy (PDT) treatment of oral lesions combined with an intraoral probe for cancer screening, incorporated here into an integrated theranostic device for image-guided PDT. **Aim**: This study aimed to validate technical performance of a novel hand-held smartphone-coupled intraoral device designed for simultaneous imaging and photodynamic therapy (PDT) of oral lesions. The imaging and PDT light delivery capabilities of the handheld system were evaluated using tissue phantoms containing protoporphyrin IX (PpIX) and a mouse model of OSCC photosensitized using 5-aminolevulinic acid (ALA)-induced PpIX. **Approach**: The probe's built-in multi-channel fluorescence and polarized white light imaging capabilities were evaluated using tissue phantoms with TiO_2 and controlled PpIX concentrations. *In-vivo* testing was performed using mice with subcutaneous TR146 OSCC implants before and after administering ALA, and again to assess photobleaching after light delivery (a total of $100 J/cm^2$ at 635 nm from the integrated diode laser). **Results**: Quantification of fluorescence images generated using the device showed that the PpIX signal scaled linearly with concentration, and the extent of photobleaching increased with increasing PDT dose as expected. In murine xenografts, PDT treatment delivered through the intraoral probe reduced tumor volume significantly in comparison to untreated control animals. **Conclusion**: Our findings demonstrate the effectiveness of a low-cost handheld device for simultaneous quantitative imaging of PpIX fluorescence and image-guided PDT in vivo. The integration of intraoral imaging and image-guided treatment into the same handheld device paves the way for a streamlined approach to cancer screening and early intervention with PDT at the point of care.

Keywords: Oral cancers, Smartphone, Intra-oral device, Photodynamic therapy (PDT), ALA, PpIX, Fluorescence imaging.

Correspondence to author: Jonathan P. Celli, PhD., E.mail: Jonathan.celli@umb.edu, Department of Physics, College of Science and Mathematics, University of Massachusetts Boston, Boston, Massachusetts, United States.

Optical Methods for Tumor Treatment and Detection: Mechanisms and Techniques in Photodynamic Therapy XXXII, edited by David H. Kessel, Tayyaba Hasan, Edward V. Maytin, Proc. of SPIE Vol. 12823, 1282302
 · 1605-7422 · doi: 10.1117/12.3001825

1. INTRODUCTION

Cancers of the oral cavity are among the most common malignancies worldwide, with more than 377,000 new cases and almost 178,000 deaths in 2020.[1] Incidence and mortality are particularly staggering in South Asia. In India, where chewing tobacco-based mixtures are widely popular, there are more than 100,000 cases per year. Even with screening campaigns to catch early disease, the ability to provide timely intervention at such scales is limited by inadequate penetrance of surgical oncology and radiotherapy facilities in resource-limited settings, especially in rural areas. Motivated by the unmet need for treatments that can be universally available, including to patients in low and middle-income countries (LMICs), we developed low-cost technology for photodynamic therapy (PDT) of early oral squamous cell carcinoma (OSCC).[2–9] Our approach used the photosensitizer precursor 5-aminolevulinic acid (ALA), which leads to the accumulation of protoporphyrin IX (PpIX) prior to illumination with red light, which selectively triggers lethal photochemistry in local targeted tumor tissue. Further, building on previous clinical validation, here we developed a multichannel fluorescence imaging probe for oral cancer diagnosis,[10–15] and technology for intraoral image-guided PDT of oral cavity lesions, integrated with image-guided therapy (IGT) smart device, incorporating PDT laser light delivery and imaging optics (excitation LEDs, emission filters and camera) in a unit with dental camera form factor. Preclinical assessments were done on in-vitro tissue phantoms as well as on in-vivo murine subcutaneous tumor models.

2. MATERIAL AND METHODS

2.1 *In-vitro* and *in-vivo* model and image-guided PDT timeline

In-vitro studies were conducted the intra-oral imaging/treatment device using TR146 OSCC cells. This cell line (Cat. no. ECACC 10032305) was derived from a well-differentiated keratinizing squamous cell carcinoma in the oral cavity. The cell culture was maintained in Ham's F-12K (Kaighn's) medium supplemented with L-glutamine, sodium bicarbonate buffer system, 10% FBS, 100 μg/ml penicillin/streptomycin, and 0.5 μg/ml amphotericin-B. The cells were grown in 75 cm^2 T-flasks and trypsinized (trypsin 25%) when the cell density in each flask reached 0.5 x 10^6 cells/ml. These cells were then used for further study in a 3D phantom. To generate nearly physiological PpIX fluorescence, the cells were incubated with 3 mM ALA (5-Aminolevulinic acid HCI, Sigma Aldrich, Israel) for 4 hours in a new two T-flask. The cells were then pelleted down after a 5-minute centrifugation at 5000 rpm. After centrifugation, the cells were dissolved in 30 μl of TiO_2 and pipetted into a 2% (w/v) sodium alginate hydrogel phantom. The hydrogel was crosslinked using DPBS supplemented with Ca^{2+} and Mg^{2+} ions. The fluorescence intensities of PpIX were measured at different concentrations of PpIX (0-50 μg/ml) in TiO_2 (0.58 g/l) tissue phantom, which were previously calibrated.[2,16,17]
Swiss nu/nu nude mice, males, and females, 6-8 weeks old and 20-25 grams, were obtained from Charles River Laboratories in Waltham, MA. Our research method at the University of Massachusetts Boston involved using an established subcutaneous tumor model to create relatively uniform tumor masses on a controlled schedule. The mice were anesthetized using isoflurane inhalation during the subcutaneous implantation. 6×10^6 TR146 cells in a 50 μl volume (1:1; Ham's F-12K, Matrigel® Matrix with growth factor reduced) injected subcutaneously into the right flank of each mouse. The tumors were allowed to grow until they reached about 5 mm in diameter, which took approximately 10 days after implantation. We administered ALA (200mg/kg) intratumorally, which resulted in PpIX accumulation at the tumor site after 2.5 hours. Here, intratumoral ALA administration was used to model a local topical photosensitization protocol[18] The intraoral device incorporated a 635 nm laser light was used for PDT treatment (total dose 100J/cm^2). Post-PDT tumor response was evaluated for a total of 10 days. Prior to tumor implantation, treatment, and monitoring, the mice were anesthetized by isoflurane inhalation, and tumor size was measured with a digital vernier caliper. At the end of the experiments, the tumor was excised from the sacrificed mice, weighed, measured, and processed for histopathology analysis.

2.2 Handheld intraoral imaging and PDT light delivery device

The integrated intra-oral device is an upgraded version of a previous mobile imaging device with a semi-flexible intraoral probe, which has successfully demonstrated functionality, diagnostic performance, and clinical ease of use in LMICs.[4,11,13–15] Here, we incorporated laser light delivery for PDT into the same overall dental-camera style physical form as the previous handheld diagnostic system. The overall optical design has one micro-camera and 3 different light sources. Figure 1 represents the components of the handheld intra-oral device. The system

parameters for this device are summarized in Table 1. Briefly, one camera captures polarized white light images. Here, white light LED provides illumination for polarized white light images, which provide detailed surface information of the oral tissue. The second camera captures PpIX fluorescence, autofluorescence, and post-PDT photobleached surface images (excited at 405 nm). To obtain sufficient resolution over the large field of view in the oral cavity, the probe tip has the low-cost, high-performance 5-megapixel OV5648 CMOS sensor with 2592x1944 pixels (OmniVision Technologies Corp). Similar to the 3rd generation prototype, one polarizer is added in front of each white LED to provide polarized illumination, and another polarizer will be placed in front of the imaging optics to remove the specular reflection. To capture an autofluorescence image, a long-pass filter, which only passes the light with a wavelength longer than 450nm, is placed in front of the imaging optics to block the illumination light from UV LEDs with a center wavelength of 405nm (a short-pass filter placed in front of each UV LED reduces excitation light leakage).

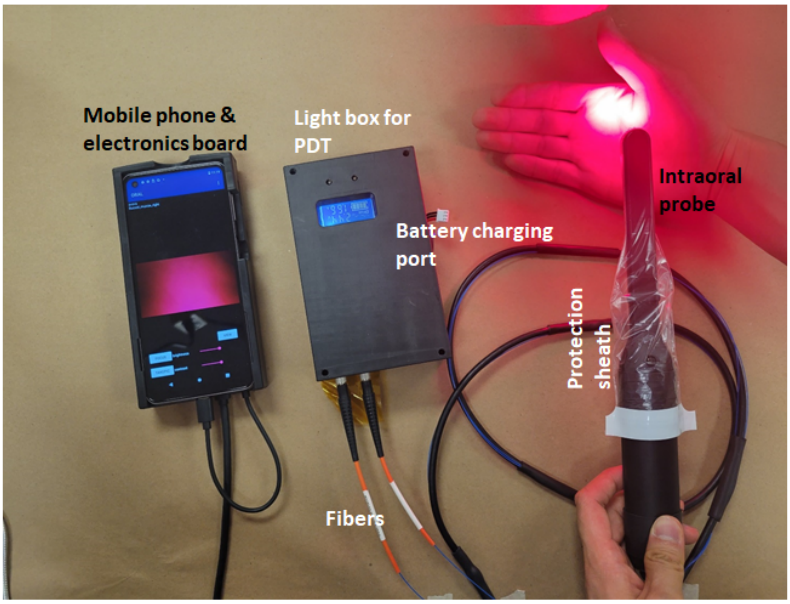

Figure 1. Photos of the intraoral device, electronics board, lightbox, and handheld intraoral probe. The lightbox houses a rechargeable battery, two diode lasers, and a current regulator. This regulator provides data on the driving current and voltage. The battery can be recharged via an integrated USB connector. The handheld probe has an autofocus camera module, which can operate in two distinct imaging modes: autofluorescence and polarized white light.

The lightbox for PDT has a rechargeable battery, two 635 nm diode lasers (though only one will be needed, based on our initial testing), and a current regulator. The red light from the laser diode is coupled to two 1.5mm diameter multimode fibers. At the tip of the probe head, two mirrors are used to direct the light from the fibers to the tissue surfaces. To achieve minimum target irradiance, the total optical power from the fiber (accounting for beam expansion and mirror losses) is > 160 mW).

3. RESULTS AND DISCUSSION

3.1 *In vitro* device performance evaluation

The device's imaging capabilities were initially evaluated using tissue phantoms with a range of concentrations of protoporphyrin IX (PpIX, the relevant photoactive compound that accumulates in tissue after ALA photosensitization). For these measurements, the intraoral probe was held above samples at a fixed distance during imaging and PDT treatment procedures, as shown in Figure 2. Tissue phantoms were prepared by mixing PpIX at specified concentrations with and without titanium dioxide as a standard scattering agent. The power output of red laser diode emission for PDT treatment (Figure 2c) was measured to be 150 mW at each of the 2 fiber ports; treatments performed below used only one fiber coupling. Using the approach described above, the

Table 1. Intra-oral device characteristics and performance metrics.

Parameters	**Fluorescence imaging**	pWLI	PDT
Light source	UV LED	White LED	Diode laser
Detector	CMOS sensor	CMOS sensor	N/A
Spectral output (nm)	405	450-650	635
Detection spectrum (nm)	450-650	450-650	N/A
Working distance (mm)	10-40	10-40	N/A
Field of View (at 25mm working distance (mm)	30X20	30X20	30X20
Lateral resolution(um)	25	25	N/A
Irradiance at lesion surface(mW/cm^2)	Tunable	Tunable	>30

linearity of the fluorescence signal was established in PpIX solutions and a highly scattering phantom. Overall performance was excellent with nearly perfect linearity with PpIX concentration in solution and strongly linear over physiologically relevant concentration range in phantoms (Figure 3a). The device was also capable of detecting PpIX fluorescence in oral squamous cell carcinoma (OSCC) cell culture aggregates that were incubated with ALA to produce endogenous protoporphyrin IX relative to control samples(Figure 3b).

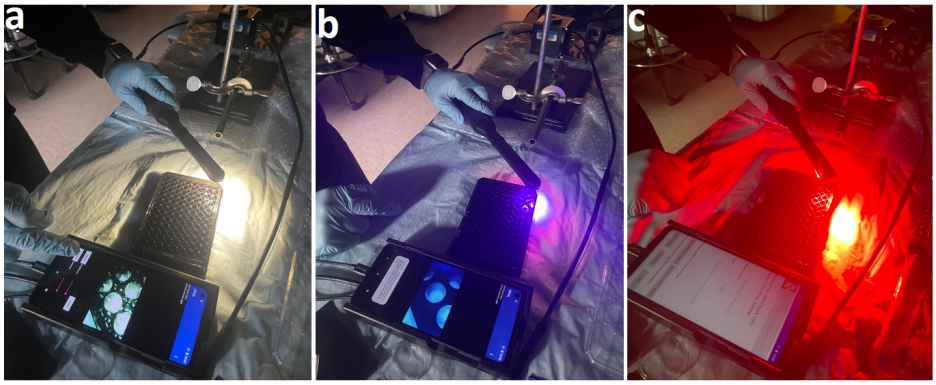

Figure 2. Device testing in tissue phantoms and cell cultures using (a) white light imaging, (b) multichannel fluorescence imaging, and (c) PDT light delivery.

An important capability of the intra-oral device is the ability to measure PpIX photobleaching, the drop in fluorescence that occurs when any fluorescent dye is exposed to light and is significant in PDT, where the extent of photobleaching can be used as a surrogate reporter of dose deposited in tissue. This is an important feature of the device for monitoring PDT treatment, potentially in real-time going forward. Agarose-based tissue phantoms were prepared, imaged using white light and fluorescence, treated using the red light PDT light delivery function, and then imaged again using the device (Figure 3c). For PDT treatments, the device was positioned above the target tissue and calibrated to deliver an irradiance of $150mW/cm^2$ at the target site to deposit the total indicated light dose of $50J/cm^2$ or $100J/cm^2$. For PDT treatments, the beam quality was found to be improved (more homogenous) by the use of a slide-on beam diffuser over the light delivery head, which does not cover the camera or fluorescence excitation optics. Photobleaching after PDT light delivery was evident visually and from quantification of device image data (Figure 3c, d). We also used the device to assess the depth of photobleaching by cutting tissue phantoms and rotating them 90 degrees. The 2.2 mm depth of photobleaching is consistent with expectations for such an optically opaque sample (data not shown).

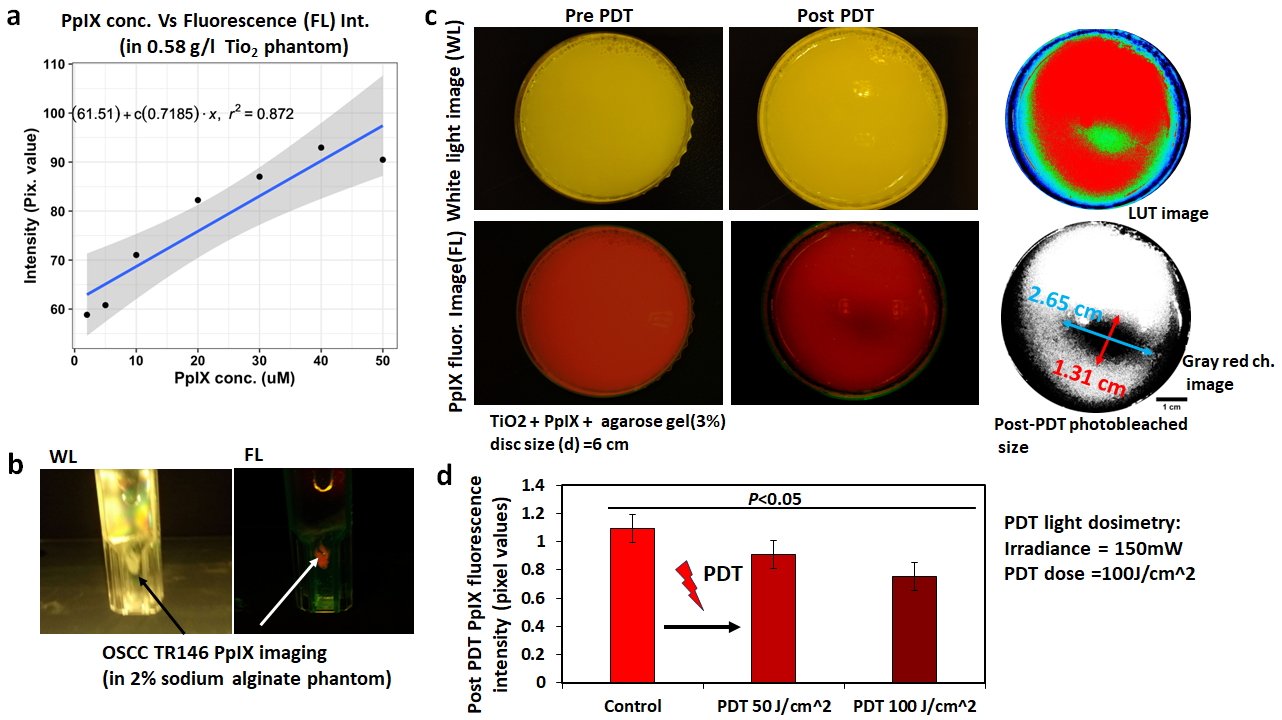

Figure 3. Linearity of PpIX fluorescence signal in tissue phantoms containing TiO_2 to simulate scattering (a). Detection of PpIX fluorescence in ALA photosensitized OSCC cultures is shown in (b). Evaluating the device capability for imaging PpIX photobleaching as a corollary of PDT dose deposited in tissue (c, d).

3.2 Device performance evaluation in mouse models

Having established key performance parameters in vitro, further device assessment was carried out in mouse tumor xenografts (Figure 4a, timeline). Here, multichannel fluorescence imaging plays an important role in imaging tissues from a live animal with a significant autofluorescence background. Immune-compromised athymic Swiss Nu/nu mice were used for these studies. TR146 OSCC cells were prepared in culture, harvested, and implanted subcutaneously (5 million cells) into the flank of each animal and allowed to grow for 7-9 days to form mature tumors prior to imaging and treatment. The capability of the MOST device to longitudinally image animals to confirm photosensitization after ALA relative to before ALA injection and comparing photobleaching expected to occur after light delivery to the target tumor were all evaluated here. Prior to ALA injection (Figure 4b), the green fluorescence signal is qualitatively dominant as expected from endogenous autofluorescence. After injecting ALA, the red fluorescence signal becomes dominant from the conversion of ALA into PpIX corresponding to photosensitization, which provides the device user with real-time confirmation that treatment is ready to proceed. In this case, the skin was surgically pulled back from the tumor to confirm tumor fluorescence (Figure 4c, d). Further comparative analysis was carried out on tumors resected from animals that had not received ALA injection. This confirmed that the fluorescence signal is predominantly green in the absence of ALA photosensitization (data not shown).

Finally, a separate batch of tumor-bearing animals was assigned for photosensitization and going on to receive PDT treatment without undergoing terminal resection at the time of imaging. Quantification of the intensity of PpIX fluorescence signal in images obtained after photosensitization and treatment (photobleaching), confirming the expected time trend where bleaching quenches fluorescence signal back to approximately pre-photosensitization level a promising indicator that treatment was successful (data not shown). These animals received PDT light delivery after 2.5 hours ALA (200 mg/kg) intra-tumoral injection and tumor volume ($\pi/_6(l \cdot w \cdot h)$) monitored using digital calipers to measure tumor dimensions every day to assess the response to PDT delivered via device continuing in time about 7 days (Figure 4e). The percentage change in tumor size

reduced to the 6th day post-PDT compared to control mice, where tumor size increased to 4.5 times (mean value).

Overall, the performance tests confirmed that the device functions as an integrated device for PpIX/autofluorescence imaging and PDT treatment while preserving the physical form factor of an intraoral camera, as designed.

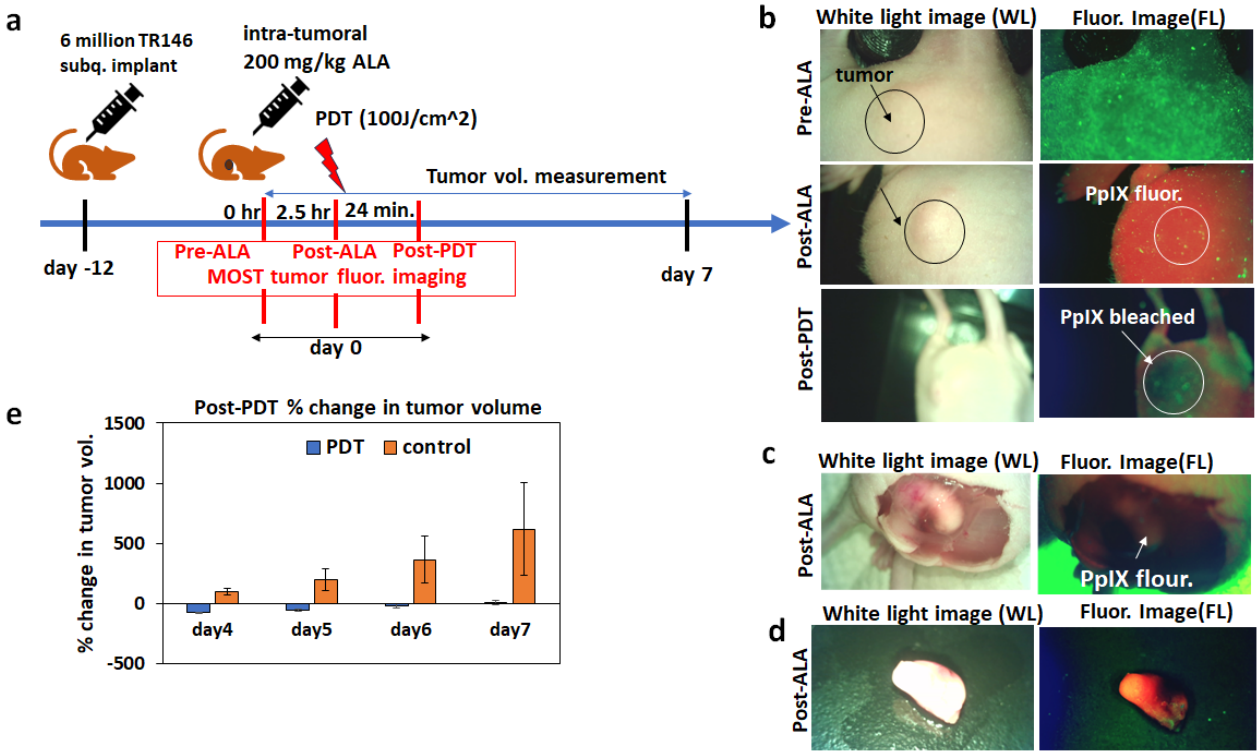

Figure 4. In vivo imaging and PDT using the intraoral device in murine tumor xenografts. The timeline (a) shows that mice were implanted with TR146 cells, forming mature tumors 5-7mm in diameter over 12 days prior to PDT treatment. On the treatment day, mice were assigned to either receive PDT treatment or to a no-treatment control group. PDT-treated mice were photosensitized by intratumoral injection of ALA. Device-mediated imaging was conducted before and after ALA photosensitization and immediately after PDT. (b) Longitudinal volume measurements were obtained using digital calipers at time points up to 7 days post-treatment. Untreated tumors continued to undergo volume doublings, while PDT-treated animals exhibited tumor reduction within the first 5 days and no measurable regrowth over the duration of the study. (c) The pre-ALA tumor site shows skin auto-fluorescence, which, upon PDT treatment, departs photo-bleached. (d) The post-ALA administered tumor (after 2.5 hours) shows PpIX fluorescence.

4. CONCLUSION

Here, we validated the performance of a handheld probe for simultaneous intraoral imaging and PDT light delivery, bringing together two previously separate technologies into a single handheld device. This portable and lightweight device is battery-powered. It retains previous cancer screening functionality, in which autofluorescence and white light images can be analyzed through cloud-linked remote diagnosis. The combination of these advanced technologies has the potential to enhance the accuracy and efficiency of diagnosing and treating oral health conditions (malignant and pre-malignant) in areas that have limited access to medical resources. As a PDT treatment technology, the same hardware can be leveraged for light delivery under simultaneous fluorescence image guidance. Further software development is in progress leveraging the capability to monitor photobleaching for real-time treatment monitoring.

ACKNOWLEDGMENTS

We gratefully acknowledge funding from the NIH/NCI, U01 CA279862 (to JPC, TH and RL).

REFERENCES

[1] Sung, H., Ferlay, J., Siegel, R. L., Laversanne, M., Soerjomataram, I., Jemal, A., and Bray, F., "Global cancer statistics 2020: Globocan estimates of incidence and mortality worldwide for 36 cancers in 185 countries," *CA: a cancer journal for clinicians* **71**(3), 209–249 (2021).

[2] Hempstead, J., Jones, D. P., Ziouche, A., Cramer, G. M., Rizvi, I., Arnason, S., Hasan, T., and Celli, J. P., "Low-cost photodynamic therapy devices for global health settings: Characterization of battery-powered led performance and smartphone imaging in 3d tumor models," *Scientific reports* **5**(1), 10093 (2015).

[3] Khan, S., Hussain, M. B., Khan, A. P., Liu, H., Siddiqui, S., Mallidi, S., Leon, P., Daly, L., Rudd, G., Cuckov, F., et al., "Clinical evaluation of smartphone-based fluorescence imaging for guidance and monitoring of ala-pdt treatment of early oral cancer," *Journal of biomedical optics* **25**(6), 063813–063813 (2020).

[4] Khan, S., Song, B., Mallidi, S., Li, S., Liu, H., Bilal Hussain, M., Siddiqui, S., Khan, A. P., Akhtar, K., Siddiqui, S. A., et al., "Clinical assessment of a low-cost, hand-held, smartphone-attached intraoral imaging probe for 5-aminolevulinic acid photodynamic therapy monitoring and guidance," *Journal of Biomedical Optics* **28**(8), 082809–082809 (2023).

[5] Liu, H., Daly, L., Rudd, G., Khan, A. P., Mallidi, S., Liu, Y., Cuckov, F., Hasan, T., and Celli, J. P., "Development and evaluation of a low-cost, portable, led-based device for pdt treatment of early-stage oral cancer in resource-limited settings," *Lasers in surgery and medicine* **51**(4), 345–351 (2019).

[6] Liu, H. and Celli, J. P., "Looking out the optical window: Physical principles and instrumentation of imaging in photodynamic therapy," in [*Imaging in Photodynamic Therapy*], 25–50, CRC Press (2017).

[7] Mallidi, S., Mai, Z., Rizvi, I., Hempstead, J., Arnason, S., Celli, J., and Hasan, T., "In vivo evaluation of battery-operated light-emitting diode-based photodynamic therapy efficacy using tumor volume and biomarker expression as endpoints," *Journal of biomedical optics* **20**(4), 048003–048003 (2015).

[8] Mallidi, S., Khan, A. P., Liu, H., Daly, L., Rudd, G., Leon, P., Khan, S., Hussain, B. M., Hasan, S. A., Siddique, S. A., et al., "Platform for ergonomic intraoral photodynamic therapy using low-cost, modular 3d-printed components: design, comfort and clinical evaluation," *Scientific reports* **9**(1), 15830 (2019).

[9] Siddiqui, S. A., Siddiqui, S., Hussain, M. B., Khan, S., Liu, H., Akhtar, K., Hasan, S. A., Ahmed, I., Mallidi, S., Khan, A. P., et al., "Clinical evaluation of a mobile, low-cost system for fluorescence guided photodynamic therapy of early oral cancer in india," *Photodiagnosis and Photodynamic Therapy* **38**, 102843 (2022).

[10] Figueroa, K. C., Song, B., Sunny, S., Li, S., Gurushanth, K., Mendonca, P., Mukhia, N., Patrick, S., Gurudath, S., Raghavan, S., et al., "Interpretable deep learning approach for oral cancer classification using guided attention inference network," *Journal of biomedical optics* **27**(1), 015001–015001 (2022).

[11] Song, B., Sunny, S., Li, S., Gurushanth, K., Mendonca, P., Mukhia, N., Patrick, S., Gurudath, S., Raghavan, S., Imchen, T., et al., "Mobile-based oral cancer classification for point-of-care screening," *Journal of biomedical optics* **26**(6), 065003–065003 (2021).

[12] Yang, S. M., Song, B., Wink, C., Abouakl, M., Takesh, T., Hurlbutt, M., Dinica, D., Davis, A., Liang, R., and Wilder-Smith, P., "Performance of automated oral cancer screening algorithm in tobacco users vs. non-tobacco users," *Applied Sciences* **13**(5), 3370 (2023).

[13] Song, B., Sunny, S., Uthoff, R. D., Patrick, S., Suresh, A., Kolur, T., Keerthi, G., Anbarani, A., Wilder-Smith, P., Kuriakose, M. A., et al., "Automatic classification of dual-modalilty, smartphone-based oral dysplasia and malignancy images using deep learning," *Biomedical optics express* **9**(11), 5318–5329 (2018).

[14] Uthoff, R. D., Song, B., Sunny, S., Patrick, S., Suresh, A., Kolur, T., Keerthi, G., Spires, O., Anbarani, A., Wilder-Smith, P., et al., "Point-of-care, smartphone-based, dual-modality, dual-view, oral cancer screening device with neural network classification for low-resource communities," *PloS one* **13**(12), e0207493 (2018).

[15] Birur N, P., Song, B., Sunny, S. P., Mendonca, P., Mukhia, N., Li, S., Patrick, S., AR, S., Imchen, T., Leivon, S. T., et al., "Field validation of deep learning based point-of-care device for early detection of oral malignant and potentially malignant disorders," *Scientific Reports* **12**(1), 14283 (2022).

[16] Pogue, B. W. and Patterson, M. S., "Review of tissue simulating phantoms for optical spectroscopy, imaging and dosimetry," *Journal of biomedical optics* **11**(4), 041102–041102 (2006).

[17] Sunar, U., Rohrbach, D. J., Morgan, J., Zeitouni, N., and Henderson, B. W., "Quantification of ppix concentration in basal cell carcinoma and squamous cell carcinoma models using spatial frequency domain imaging," *Biomedical optics express* **4**(4), 531–537 (2013).

[18] Ma, C.-H., Yang, J., Mueller, J. L., and Huang, H.-C., "Intratumoral photosensitizer delivery and photodynamic therapy," *Nano Life* **11**(02), 2130003 (2021).